

# Ceramic particles and layers for functional application

Heinrich Hofmann\*

*Powder Technology Laboratory, Ecole Polytechnique Fédérale Lausanne, CH-1015 Lausanne, Switzerland*

Available online 1 October 2008

## Abstract

Besides ‘bulk’ structural and functional ceramic, a third interesting group of inorganic or ceramic materials exists: particles used for medical applications like contrast agent as building blocks for photonic crystals, as thin or thick layers with controlled porosity or grain sizes showing interesting thermal or electrical behaviour or finally nanostructured ceramic with novel optical and mechanical properties. As high-tech ceramic this type of ceramic needs very well synthesised powders of high purity, defined sizes for the use of quantum effects and small size distributions. Very often, complex powders like core–shell particles with nanometer thin layers are needed to fulfil physical as well as biological demands. Additionally, powder processing is one of the key factors to reach outstanding structural and functional properties. Especially the stability of colloidal suspensions and the drying step during the film manufacturing are objects of the research because nanosized particles cause particular problems normally not observed with micron- or submicron-sized powders. Application of nanosized superparamagnetic iron oxide particles for molecular imaging and cancer treatment and results regarding the manufacturing of thin nanostructured layers for interesting physical (thermal conductivity) and medical (drug delivery) will be presented.

© 2008 Published by Elsevier Ltd.

*Keywords:* Powder synthesis; Ceramic layer; Nanostructured powders; Porosity; Drying; Biomedical application

## 1. Introduction

Besides structural and functional ceramic, a third interesting group of inorganic or ceramic materials exists: particles used for medical applications like contrast agent, for drug delivery, cancer treatment or adjuvant for vaccination, as building blocks for photonic crystals, as thin or thick layers with controlled porosity or grain sizes showing interesting thermal or electrical behaviour or finally nanostructured ceramic with novel optical and mechanical behaviour. The common thing with technical ceramic is the use of the same or at least similar raw material, like sub-micrometric powders and similar processing technologies whereas colloidal processing is the most important. The important difference is that the grain size in the final application is very often sub-micrometric and consolidation steps like sintering are not always necessary to get the final product. The knowledge in ceramic technology enables the use of inorganic powders in high-tech areas like drug delivery, batteries, data storage, sensors and finally also in smart materials.

High-tech ceramic needs very well synthesised powders of high purity and small size distributions. Powder processing is

one of the key factors to reach outstanding structural and functional properties. The new trend of research and development as mentioned above needs more sophisticated powder with properties like nearly monosized nanopowders showing quantum effects, easy to disperse and very often with complex morphologies like core–shell particles with nanometer thin coatings. Such powders are processed to monolayers and/or ordered arrangement of particles in a large area and this in 0–3 dimensions. This paper starts by describing developments in particle synthesis and processing for this new type of applications and examples like nanosized multifunctional particles with superparamagnetic behaviour and quantum effects embedded in a silica matrix will be presented.

## 2. Particle synthesis

The synthesis of powders with controlled shape, narrow particle size distributions, desired stoichiometry and crystal polymorph is still a major concern for many applications. This is the case especially for powders for functional ceramics and particularly for nano-effects like fluorescence or superparamagnetic. Lab-scale production as normally presented in research journals are very difficult to scale-up and the developed materials and processes could very often not fulfill the eco-

\* Tel.: +41 21 6933607.

E-mail address: [heinrich.hofmann@epfl.ch](mailto:heinrich.hofmann@epfl.ch).

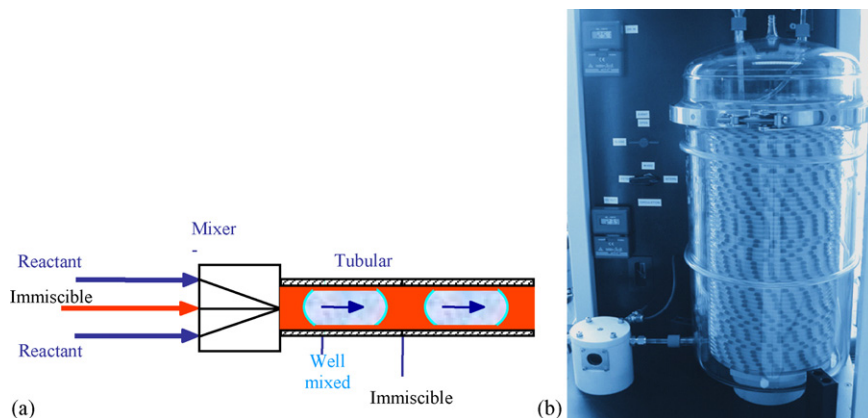


Fig. 1. Segmented tubular flow reactor. (A) Scheme of the mixing and segmentation; (b) reactor for the production of several kg powders per day.

nomic challenges. The segmented flow tubular reactor (SFTR) overcomes many of the problems often encountered when using batch reactors with respect to product quality and process efficacy (Fig. 1). The SFTR is composed of a mixer integrated into a segmenter and a tubular reactor. A supersaturation is created in the mixing chamber inducing the precipitation of particles. The precipitating suspension is then segmented into identical small volumes by forming droplets in a non-miscible fluid. The SFTR achieves a quasi-plug flow when compared to large batch volumes; the micro-volumes created in the SFTR are more homogeneous. The main reason for the improved homogeneity in phase composition and chemical composition is the fact that the nucleation of the primary crystals is controlled by seeds or by homogeneous nucleation. Fouling and other sources for uncontrolled nucleation are eliminated in this reactor. The precipitated product is consequently more homogeneous with narrower particle size distributions, enhanced control of particle morphology, polymorph selectivity and better stoichiometric control; all these features have been demonstrated.<sup>1</sup> To increase productivity for commercial application the SFTR can be “scaled-out” by multiplying the number of tubes running in parallel instead of scaling-up by increasing their size. Examples for calcium carbonate and barium titanate, produced using this technology will be presented illustrating a scaling-out factor of 5000 with no change in product quality and the robustness of ultrafine barium titanate powder quality.

Process control of any precipitation reaction strongly depends on the knowledge of the precipitation mechanism. Recent results on the kinetics and growth mechanisms for the both the nanostructured calcite<sup>2</sup> and nanosized barium titanate<sup>3</sup> illustrate this.

The precipitation of calcium carbonate has been studied for many years to control particle size and the crystalline phase an additive is often used. In the present study both seeds and polyacrylic acid (PAA) were added to a potassium carbonate solution (0.02 moles/L) and precipitation was carried out by mixing with calcium nitrate solutions (0.02 moles/L). Typical calcium carbonate particles have a slightly elongated shape but were pure calcite within the detection limits of X-ray powder diffraction (Fig. 2a). The powders have specific surface areas around 35 m<sup>2</sup>/g and XRD line broadening shows crystallite sizes around 60 nm. The particle size distribution for the mini-batch, the single tube SFTR and multi-tube SFTR precipitates shown in Fig. 2b are very similar.

The barium titanate precipitation was carried out using barium hydroxide and titanium tetrachloride. A series of batches of several kg were produced. The precipitated barium titanate showed primary particle sizes between 50 and 200 nm (Fig. 3a). The particle size distributions measured using the XDC for nine different lots are shown in Fig. 3b.

These two examples show that the segmented flow tubular reactor is a robust technology well suited to process intensification without the loss of product quality. The SFTR creates small

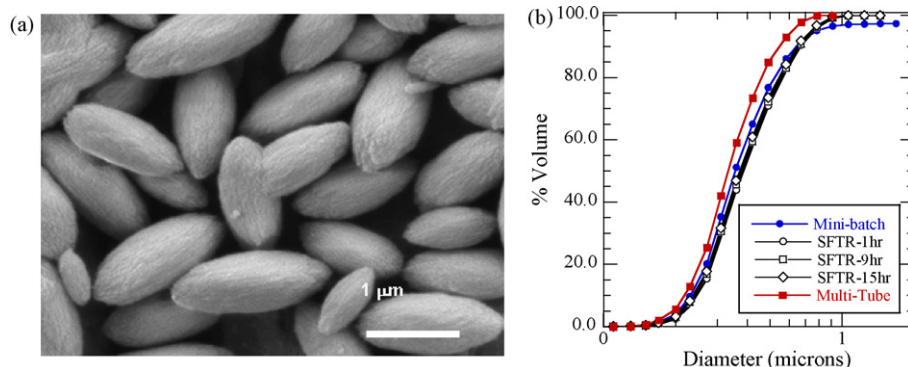


Fig. 2. Calcium carbonate precipitated in the segmented tubular reactor in the presence of polyacrylic acid (PAA). (a) Scanning electron micrograph of the powder particle (sample taken after 9 h production) and (b) particle size distributions for mini-batch, single tube SFTR and multi-tube configuration.

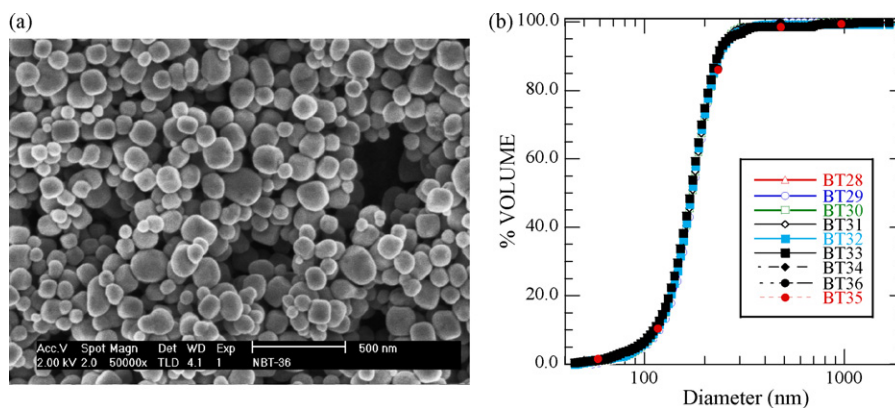


Fig. 3. Barium titanate powder using SFTR technology. (a) Scanning electron micrograph and (b) PSDs measured using XDC cumulative volume distributions for nine different lots.

reaction volumes in a tubular reactor that can be operated in a continuous manner.

For application in the field of medicine, bioengineering and sensors, particles with a homogeneous composition are important, and additional properties like magnetism, fluorescence, biocompatibility and specific adsorption behaviour at the surface have to be built into the particles. Such multifunctional particles are always composite particles because the different physical properties could be only fulfilled with different nanoparticles inside a larger (still smaller than 500 nm) beads. Typical applications such as various separation techniques and MRI contrast agents are relatively well established on the market, whereas drug delivery and targeting is still in a development stage.<sup>4</sup> Sev-

eral studies on multifunctional particles have been published, mostly produced by layer-by-layer assembly of polymers and particles.<sup>5</sup> The layer-by-layer technique is a very labor-intensive and time-consuming technique due to consecutive purification of the sample. In addition high loading of nanoparticles in the beads can be achieved only by subsequent assembly of nanoparticles onto the surface of the beads.

To overcome these disadvantages an inverse microemulsion method, with a water/prehydrolyzed tetramethylorthosilicate (TMOS)/nanoparticle mixture in octane, stabilized by an anionic surfactant (sodium dioctyl sulfosuccinate, AOT) for the production of highly loaded silica beads containing different kinds of nanoparticles was developed (Fig. 4).<sup>6</sup> The silica and Fe

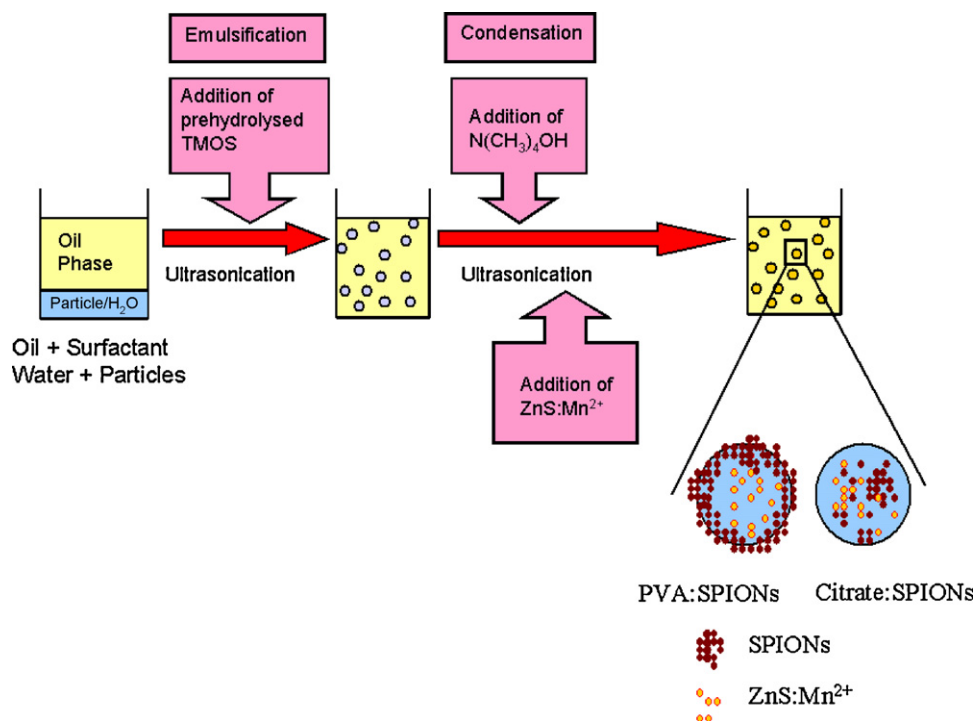


Fig. 4. Schematic illustration of the bead forming process: octane, surfactant, water, and nanoparticles are emulsified to which prehydrolyzed TMOS is given. By addition of the base, N(CH<sub>3</sub>)<sub>4</sub>OH, condensation of the emulsified TMOS is initiated. With this technique, depending on the surface coating of the initial nanoparticles, PVA-coated SPIONs or citrate stabilized SPIONs, and their distribution in the emulsion, different kinds of nanoparticle beads and multifunctional beads can be produced.

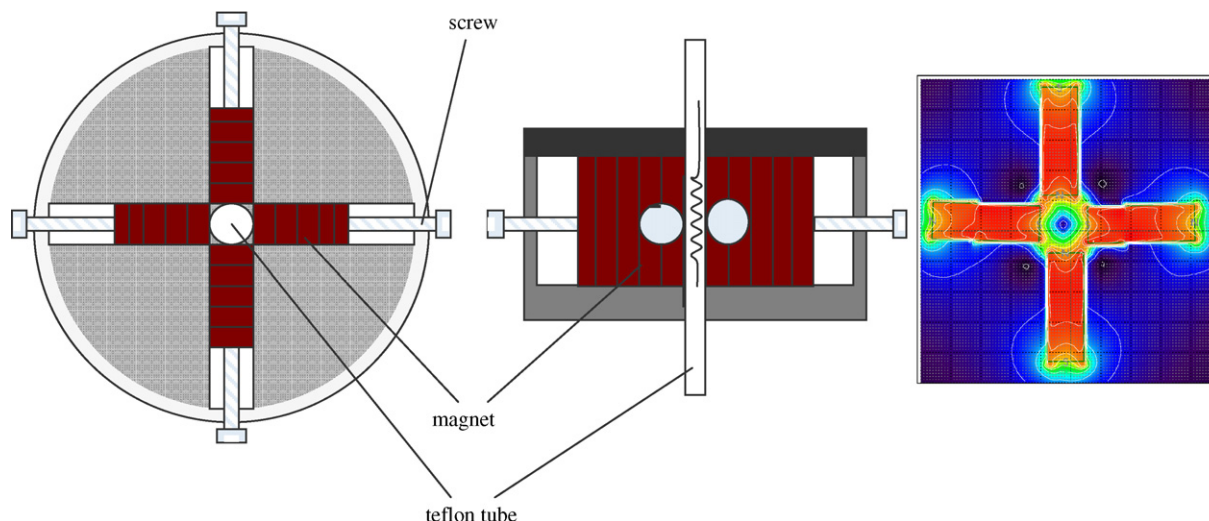


Fig. 5. Layout of the fixed bed reactor for the surface modification of superparamagnetic nanoparticles and multifunctional beads. Left: arrangement of the magnets; right: distribution of the magnetic field strengths. The max field is 600 mT and the radial field gradient inside the tube 300 T/m.

composition inserted in the synthesis can be found quantitatively in the resulting particles. The partition of the primary nanoparticles in the resulting silica/nanoparticle composite beads can be controlled by altering their surface coating. Stabilization of the iron oxide nanoparticles, which are normally called superparamagnetic iron oxide nanoparticles (SPION), by PVA resulted in the distribution of the SPIONs in the outer shell and stabilization of the SPIONs by citric acid resulted in partitioning of the iron oxide nanoparticles in the core of the silica beads. Additionally, fluorescent and magnetically separable beads were created. ZnS:Mn<sup>2+</sup> nanoparticles were co-encapsulated with the SPIONs, which were retaining their typical fluorescence spectra for low concentrations of iron oxide particles added.

For the final coating of multifunctional particles with biocompatible polymers, peptides or plasmids, normally a multistep liquid phase synthesis is used. This process is time consuming and laborious because each addition reaction on the particle surface is followed by a purification step such as magnetic sedimentation, size exclusion chromatography, or dialysis. Although ultrasonication is often applied to dissociate the bead agglomerations, it may cause damage to the bound bio-active molecules, resulting in an overall decrease of their biological activity. In order to bypass the need for repeated purification and to assure continuous working processes for the surface modification of nanosized SPION or beads (iron oxide in silica or the above mentioned multifunctional particles), we immobilized SPIONs as a stationary solid phase in a column by a high gradient permanent magnetic field. For functionalization of the immobilized particles during solid phase synthesis the chemical reagent is conducted over the SPIONs as solid support. Although solid phase synthesis on polymer support is widely described, to our knowledge the solid phase multistep biofunctionalization of SPIONs in a magnetic fixed bed reactor is novel.<sup>7</sup> In this magnetic fixed bed reactor the immobilization of the magnetic particles is based on the attractive force exerted by a magnetic field gradient (Fig. 5). Our data indicated that the efficiencies, product qualities, especially the low agglomeration, and recovery rates of the

functionalized nanoparticles produced by solid phase synthesis were superior to those obtained by synthesis in the normal liquid phase.

### 3. Application of functionalized inorganic particles in diagnosis and therapy

#### 3.1. Imaging

Magnetic resonance imaging (MRI) has become a major, promising research topic worldwide because of its numerous potential applications (e.g. improved anatomic depiction, lesion characterization, study of blood flow changes in tissues, generation of pH maps, studies of vascular volume or permeability, denoting of gene expression, etc.). SPIONs commonly exhibit specific uptake by macrophage-like cells, explaining why – provided they are not entirely captured by liver and spleen at first-pass – they are widely investigated as MRI markers for the diagnosis of inflammatory and degenerative disorders associated with high macrophage phagocytic activity.<sup>8</sup> It was shown that superparamagnetic iron oxide nanoparticles have been successfully used for MRI of atherosclerotic plaques. Endocytosis into monocytes/macrophages has been proposed as the mechanism for SPION uptake, but a specific receptor has not been identified yet.

#### 3.2. Drug delivery and gene transfection

This activity is motivated by the clinical need for a selective targeting of drugs and improved precise control of drug delivery kinetics, especially for drugs with low bioavailability, therapeutic indices, solubility and circulating half-time. This can only be accomplished using the unique properties of superparamagnetic iron oxide particles only available in their nano-scale structures. The polymeric coating component in overall development provides versatile chemical functionalization to optimize both drug delivery dosage regimens for local drug therapy and the ligands

for targeting modes as well. SPION particles were successfully used intra-articularly and peri-articularly in experiments (24 h to 5 days) in the carpal and stifle joint of experimental sheep.<sup>9–11</sup> The use of SPION for drug delivery or gene transfection *in vivo* needs also investigations regarding the clearing of the particles “after use”. The clearing was investigated in sheep and we are able to show that the particles clear the body via spleen and kidneys as well as the liver without any sign of inflammation or other problems. Particles coated with PVA injected into the joint needs 4–5 weeks to leave the body.

### 3.3. Hyperthermia

The application of superparamagnetic iron oxide nanoparticles for therapeutic applications are still under investigation. Such applications have exploited two major advantages of iron oxides: their low toxicity to human beings and their high magnetization. For example, the magnetization is used to target drugs to the tumor area through external static magnetic fields. The tumour elimination is confined to the coupled cytotoxic drugs. If exposed to an alternating magnetic field, the harmless iron oxide particles become powerful heat sources by transforming the energy from the magnetic field into heat. Magnetic hyperthermia involves the generation of temperatures up to 43–48 °C with superparamagnetic iron oxides as particles. The treatment works by rendering cells more sensitive to radiation therapy or chemotherapy. The use of nanoparticles incorporated in an implant allows the deposition of iron oxides to be restricted to the tumor area (e.g., by intratumoral injection), thereby avoiding adverse systemic effects. The heating of magnetic oxides in an alternating-current magnetic field is mainly due to loss processes during reorientation of the magnetization or frictional losses with particle rotations in low-viscous environments. A large specific heating power is desirable to reduce the material amount to be administered to the patient. Mixtures of SPION embedded in silica microparticles were incorporated at the highest (still injectable) concentration in several embolization formulations. For *in vivo* tests Swiss nude mice were grafted subcutaneously with human colocal carcinoma Co112. The formed tumour was injected with 0.25 ml of a suspension based on poly(ethylene-co-vinyl alcohol) in dimethyl sulfoxide and containing 40% microparticles was used. The implant was injected and hyperthermia was performed for 20 min the day after, checking continuously peripheral, implanted tumoral and superficial cutaneous temperature by fluoro-optic probes. First experiments showed intratumoral equilibrium temperatures of 40.4, 43.0 and 44.5 °C with a variability of the measured temperatures smaller than  $\pm 10\%$  at 9, 10 and 10.5 mT, respectively (see Fig. 6).<sup>12</sup>

## 4. Particles for the formation of films and thick layers

### 4.1. Dip coating, drying as special problem

The most challenging production step in particular film manufacturing is drying. During drying, the systems is changing from a suspension where colloidal forces are important to a transition phase where capillary forces play a dominant role and

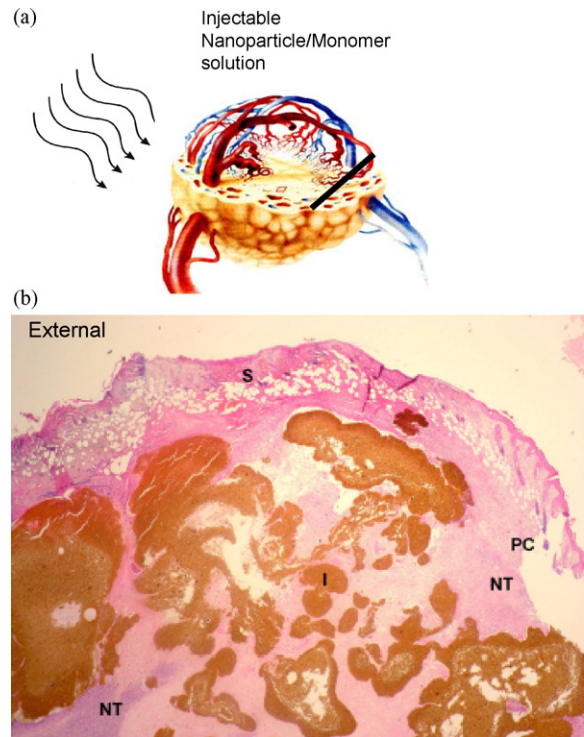


Fig. 6. Concept of magnetic hyperthermia using superparamagnetic iron oxide nanoparticles in a monomer suspension and injected into the tumor. (a) Concept, (b) histological cut through a tumor with the polymer/SPION implant (brown color). (For interpretation of the references to color in this figure legend, the reader is referred to the web version of the article.)

finally a porous solid with van der Waals forces as the only force which controls the interaction between the particles (gravity is not important at particle sizes  $< 500$  nm) are formed. Optical microscopy observations performed during evaporation of the solvent indicated these important stages of the drying process, as illustrated in Fig. 7. The sudden apparition of cracks and the temporary loss of transparency are the most relevant observations. This latter effect was confirmed by UV/vis spectrometry measurements, where a strong increase in absorbance at 500 nm close to the end of the evaporation process of the drying film was observed (Fig. 7e).<sup>13,14</sup> Simultaneously weight loss and the evaporation rate were measured. Three different evaporation rate periods can be identified. According to Brinker and Scherer these are the constant rate period, the first falling rate period and the second falling rate periods.<sup>15</sup> First, during the *constant rate period* the decrease in volume of the suspension is equal to the volume of liquid lost by evaporation, i.e. the rate of evaporation per unit area of the drying surface is independent of time. Also, at that stage, adsorption and capillary forces oppose exposure of the solid phase, so liquid flows from the interior to replace the one that evaporates. The tension in the liquid is related to the radius of curvature of the meniscus. The tension in the liquid is supported by the solid phase, which therefore goes into compression and porosity is decreasing. During this drying stage, the rising capillary pressure forces the particles to rearrange into closer packing, which is initially easy because of the flimsy structure of the network. As shrinking proceeds, the particles ultimately become too crowded to be rearranged further,

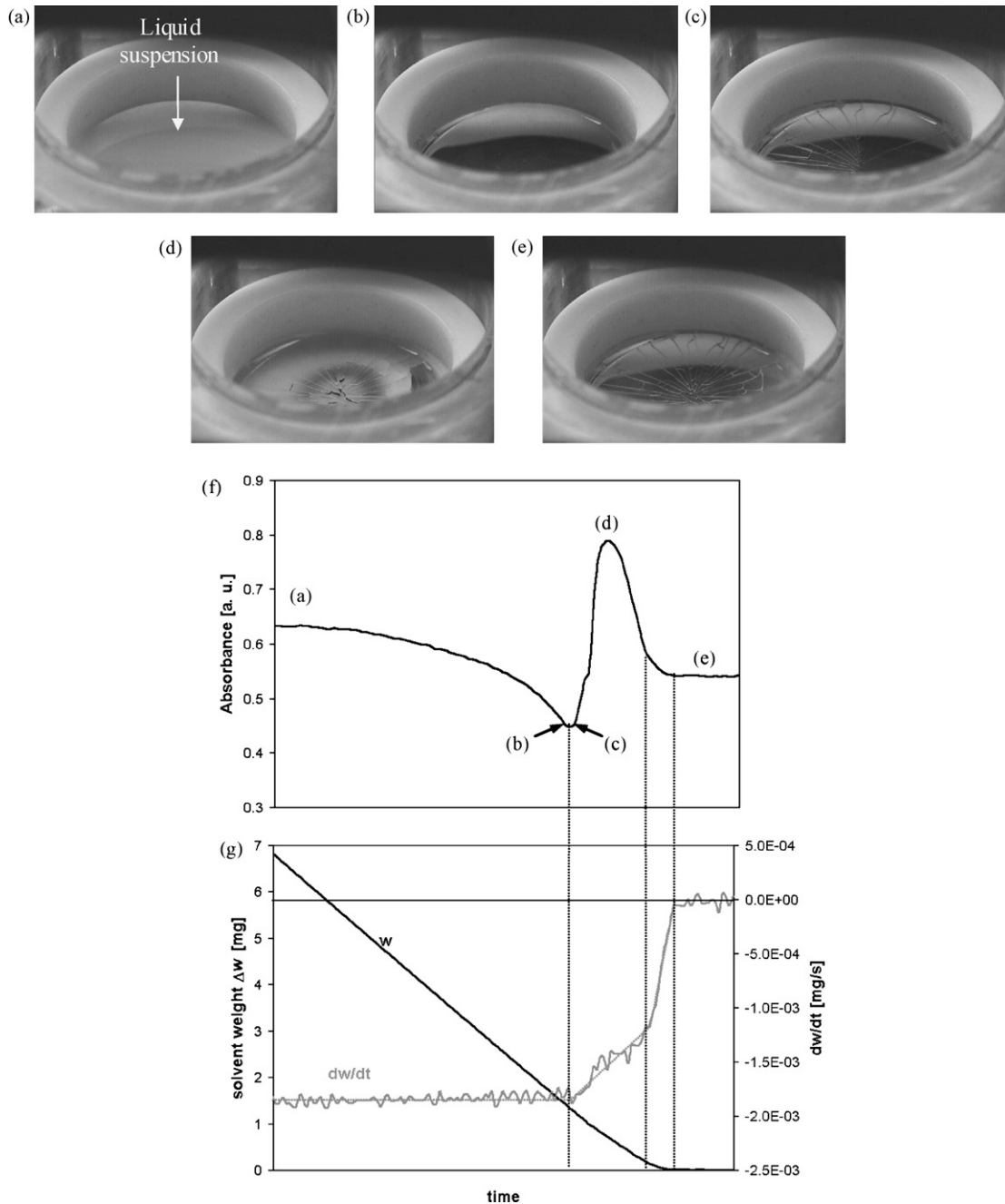


Fig. 7. In situ investigations on the experimental drying process. (a) Initial deposition of 100  $\mu\text{l}$  of the 75 nm silica suspension (0.36 g/ml) in the Teflon ring cell, (b) final snapshot before cracking, (c) first cracks propagating in the film, (d) temporary loss of transparency, (e) dry film. (f) Evolution of absorbance versus time at wavelength of 500 nm observed spectrophotometry. This latter clearly indicates the effect of sudden opacity of the film, close to the end of the drying process (after Ref. 13).

i.e. the liquid cannot overcome further stiffening of the network, and shrinkage stops. This step, where the radius of curvature of the meniscus also reached its minimal value, means the end of this first drying stage, and is called the critical point of drying. The higher tension in the liquid near the outer surface makes the portion of the network shrink faster than the body as a whole, so it tends to crack. The network experiences a tensile stress that equals, in the case of a film dried on a flat, rigid substrate as presented by Scherrer.<sup>16</sup> The stress reaches its maximum value at the surface of the film and at the critical point. This is when

cracking is most likely to occur, because of the stress difference between wet and dry parts of the body as the drying front moves toward the interior of the body. The saturated body is translucent or transparent because of the similarity in refractive index of the liquid and the solid, but the lower index of air causes significant scattering of light. Finally, other than capillary forces, such as osmotic pressure, adsorption forces and electrostatic repulsion also play a role during drying. Evaporation of the liquid solvent induces a local increase of the ion concentration. In the case of a moving drying front, such as a drying droplet, flow

of ions toward the remaining liquid is then possible, and may induce agglomeration earlier than expected. After the constant rate period, the first falling rate period describes then the process of liquid flow through partially empty pores, while the second falling rate period describes the final stage of drying, when liquid can escape only by diffusion of its vapour to the surface.

## 4.2. Example

### 4.2.1. Thin porous ceramic drug eluting coatings

Successful clinical use of medical implants can often require a concurrent systemic administration of a drug such as an antibiotic. This approach has a very low level of efficacy when the target location for the drug is the surface or general area surrounding an implant. Drug delivery coatings are designed to release the required dose of drug directly to the location of implantation over a given period of time. Efficiency of the treatment is thus dramatically increased. Drug delivery coatings have been almost exclusively built upon polymer matrix systems: biodegradable, bio-erodible, or inert. While these systems have been very successful in their drug delivery role, they have often failed by long-term stent-induced thrombosis induced by the polymer coating.<sup>17</sup> To overcome these problems, thin layered, ceramic-based coating for medical implants were developed. This coating should be highly biocompatible, resistant to wear and chemical degradation and allow high drug loading and sustained release.

This coating is built upon a network of cavities, with sizes ranging from the nanometer to the micrometer scales, linked together by a tightly controlled porosity. This structure can be arranged in a predefined manner, allowing for example the loading of a drug into the coating and its release over a long period of time by using the ceramic porosity as a diffusion limiting membrane. Multilayered ceramic coatings on stainless steel have been successfully manufactured. The innovative feature of these coatings resides in reservoirs sized between 1 and 5  $\mu\text{m}$  in diameter: these can be produced either open to the external surface or embedded between two layers of meso-porous ceramic ( $\text{TiO}_2$  for example). The ceramic layer separating the reservoir from the exterior will act as a diffusion control membrane. The elution characteristics can therefore be tuned for the desired release rate by changing the porosity morphology (Fig. 8). The coating shown in Fig. 8 shows very good adhesion of the ceramic coating on the steel substrate (in this case 316L) and first cracks perpendicular to the deformation direction were detected by in situ scanning electron microscopy tests after a plastic deformation of 2%, delimitation after 10% plastic deformation. This type of coating is still in development and first animal tests are foreseen in 1–2 years.

For manufacturing, polymeric microbeads are deposited by dip coating and used as a template. This allows a very tight size distribution of the cavities. Different bead arrangements have been successfully produced to fine-tune position, density and distance between cavities. Reservoir size obtained has been in the 1–3  $\mu\text{m}$  diameter range. The meso-porous layer was manufactured by an additional dip coating of the substrate in a water-based slurry containing 20-nm sized titania powder.

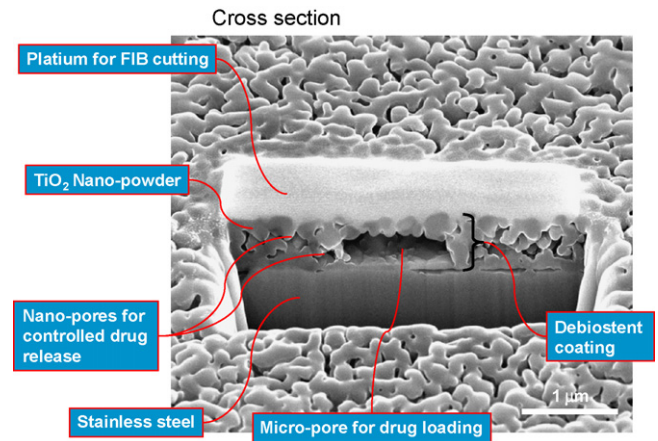


Fig. 8. Cross-section through a coated stent surface prepared by focused ion beam.

After drying, the samples were heat treated at low temperature for binder and template was burn out and finally was sintered at 800–1000  $^{\circ}\text{C}$ .

### 4.2.2. Low thermal conductivity coating on turbine blade

Coating with nanosized oxide powders opens new possibilities for tuning the thermal properties of the material. Besides the bulk properties additional features like grain boundaries, pores and crystal size in the range of the phonon wavelengths have to be in consideration for the estimation of thermal conductivity. Interesting applications of such materials are thermal barrier coatings for gas turbine blades. The temperatures under that the coatings should work are of about or exceed 1000  $^{\circ}\text{C}$ . There are two mechanisms that are important for the heat transport in non-metallic solid at such temperatures: the phonon and radiative mechanisms. Nanostructuring is assumed to decrease the phonon or photon mean free path, and so should decrease the thermal conductivity. Propagation of phonons is an important mechanism of heat transfer under high temperatures. Note that the temperature of 1000  $^{\circ}\text{C}$  exceeds the Debye temperature for most of dielectrics (e.g.,  $T_{\text{Debye}} = 769^{\circ}\text{C}$  for alumina). This means that the phonons whose wavelength is of about the lattice constant are most important for the heat transport. The commonly used continuum approximation is not appropriate to consider the inter-grain transport of these short-wavelength phonons. The model developed for heat transport in nanostructured layers assumes that the phonon and radiative part are independently of each other.<sup>18,19</sup> To investigate the high temperature phonon transport in nanostructure we assume that two mechanisms are most important: scattering at the grain boundaries and the phonon–phonon interaction. Nevertheless, for the materials whose thermal conductivity is essentially reduced due to nanostructuring the phonon scattering at the grain boundaries is of most important. This scattering determines the phonon mean free path that becomes now comparable with the grain size and is independent of the phonon wavelength.

Ceramic films were produced on steel surfaces by dip coating or electrophoretic deposition and by an additional sintering step.<sup>20,21</sup> The important parameter of the microstructure like porosity, pore size, pore size distribution, contact area between

Table 1  
Microstructure of alumina films on steel after sintering

Sample	Grain size (nm)	Deviation of grain size (%)	Porosity (%)	Pore size (nm)	Coordination number	Contact diameter (Scorohod) (nm)
FD1/1	174	36	43	300	6.45	93
FD2/2	161	16	27	310	9.2	100
FD1/3	360	16	3	570	12.1	270
FD2/1	270	20	37	280	7.0	250
FD2/2	315	15	25	200	8.9	280
FD2/3	420	15	7	350	12.1	432

the particles are used in the calculation of the thermal conductivity of such ceramic films and are given for several samples in Table 1. Fig. 9 shows the interestingly good correlation between calculated and measured thermal conductivity of porous nanostructured alumina films.

#### 4.3. Patterned coatings

Functional materials with topographically or chemically complex surfaces in the nanometer range are currently developed in view of their promising optical, catalytic or electrical properties which could find applications in biosensing or (opto-)electronic devices. The still-emerging field of nanotechnology is in need of reliable, fast, economical and versatile methods for structuring surfaces with controlled surface chemistry and topography in the nanometer range. The approach to use particles as template or functional building block and to try to arrange the particles in an ordered manner, normally as a monolayer, on the surfaces of a support, like a silicon wafer is interesting. Several principles of particles assembly are under investigation today.

One of the most straight-forward ideas is to pattern a surface with positive and negative charges. A particle suspension with, for example positively charged nanoparticles will adsorb electrostatically on the negatively charged areas and vice versa. The charged structures on the surface can be obtained via a variety of surface patterning methods known from microtechnology like micron-contact printing, charging of a surface with a focused

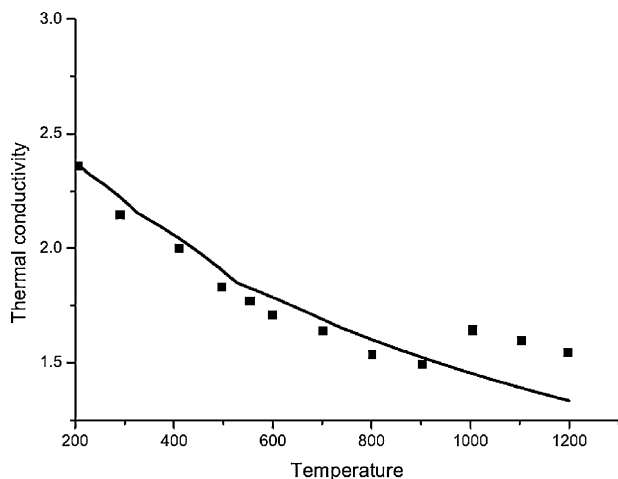


Fig. 9. Measured (points) and calculated (line) thermal conductivity (in W/mK) of sample FD2/1 of Table 1.

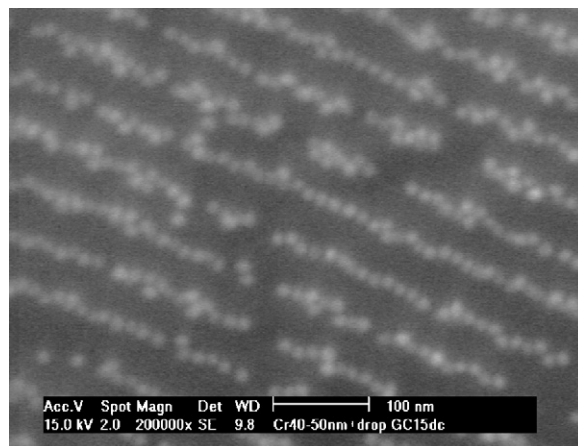


Fig. 10. SEM micrographs of chains of 15-nm gold particles obtained by drying a drop of  $5.5 \times 10^{-3}$  g/ml suspensions on a Cr nano-patterned substrates (groove width = 40–50 nm).

ion beam, photolithographically produced photoresist-surface. During drying of the solvent, it is often observed that capillary forces influence the pattern formation. The use of dip coating on topographically structured surfaces opens the way to producing large area ordered structures with a low defect density. No specific chemistry is required on the template or the particles to enable the assembly process. Therefore the methods are generic and allow a large choice of support and particulate materials. Dip coating on grooved substrates is shown to be an effective method for creating large area 1D particle arrays<sup>22</sup> (Fig. 10). 0D particle arrays were obtained by overfilling the templates (hole array) with particles followed by ultrasonic treatment. Several process parameters were varied in our experiments to again mainly understand the relative influences of the forces that play a role in the assembly process: particle–particle, particle–substrate interactions in suspension, particle diffusion toward the meniscus and capillary forces between two neighboring particles at the late stages of drying, as well as particle adhesion on a substrate at different level of immersion. Capillary forces are identified as the basis of the assembly process, but the control of the chemistry of the system is of great importance. The quality of the obtained arrays without careful optimization is a sign of the robustness of the developed techniques.

## 5. Conclusion

This short overview shows that powder synthesis and powder processing are still object of fundamental research in ceramic



science. On the other hand, these results show also that an experimental approach could lead to interesting new structures and properties. Especially the use of nanosized particles opens the door to structures and materials with novel properties. The key for both, synthesis and processing of powders is still colloidal chemistry. Only the understanding of the preparation of agglomerate free powders in slurries with a high solid content will allow the successful and economic manufacturing of interesting coatings. Our results also show, that controlled porosity combined with nanosized grains could lead to novel combination of properties of the ceramic layer using well-known ceramic manufacturing technologies.

### Acknowledgements

The author would like to thank the Swiss Federal Office for Education and Science, TOPNANO21, Swiss National Science Foundation, The Kommission für Technologien und Innovation, Switzerland and the European Community under the “Competitive and Sustainable Growth” Programme, contract G5RD-CT-1999-00123 for financial support.

P. Bowen, A. Fink-Petri, K. Dittmar and A. Tourvieille have contributed to this paper with their work and discussion.

### References

- Jongen, N., Donnet, M., Bowen, P., Lemaître, J., Hofmann, H., Schenk, R. *et al.*, Development of a continuous segmented flow tubular reactor and the “Scale-out” concept in search of perfect powders. *Chemical Engineering Technology*, 2003, **26**, 303–305.
- Donnet, M., Bowen, P., Jongen, N., Lemaître, J. and Hofmann, H., Use of seeds to control precipitation of calcium carbonate and determination of seed nature. *Langmuir*, 2005, **21**, 100–108.
- Viviani, M., Buscaglia, M. T., Testino, A., Buscaglia, V., Bowen, P. and Nanni, P., The influence of concentration on the formation of BaTiO<sub>3</sub> by direct reaction of TiCl<sub>4</sub> with Ba(OH)<sub>2</sub> in aqueous solution. *Journal of the European Ceramic Society*, 2003, **23**, 1383–1390.
- Neuberger, T., Schöpf, B., Hofmann, H., Hofmann, M. and von Rechenberg, B., Superparamagnetic nanoparticles for biomedical applications: possibilities and limitations of a new drug delivery system. *Journal of Magnetism and Magnetic Materials*, 2005, **29**, 483–496.
- Choi, W. S., Koo, H. Y., Park, J. H. and Kim, D. Y., *Journal of American Chemical Society*, 2005, **127**, 16136.
- Steitz, B., Krauss, F., Rousseau, S., Hofmann, H. and Petri-Fink, A., Positional control of superparamagnetic iron oxide nanoparticles in silica beads. *Advanced Engineering Materials*, 2007, **9**, 375–379.
- Steitz, B., Salaklang, J., Finka, A., O’Neil, C., Hofmann, H. and Petri-Fink, A., Fixed bed reactor for solid phase surface derivatization of superparamagnetic nanoparticles. *Bioconjugate Chemistry*, 2007, **18**, 1684–1690.
- von zur Muhlen, C., von Elverfeldt, D., Bassler, N. and Neudorfer, I., Superparamagnetic iron oxide binding and uptake as imaged by magnetic resonance is mediated by the integrin receptor Mac-1 (CD11b/CD18): implications on imaging of atherosclerotic plaques. *Atherosclerosis*, 2007, **193**, 102–111.
- Schulze, K., Koch, A., Petri, A., Steitz, B., Castellain, M., Hofmann, M. *et al.*, Uptake and biocompatibility of functionalized poly(vinylalcohol) coated superparamagnetic maghemite nanoparticles by synovialocytes in vitro. *Journal of Nanoscience and Nanotechnology*, 2006, **6**, 2829–2840.
- Kamau, S. W., Hassa, P. O., Steitz, B., Petri-Fink, A., Hofmann, H., Hofmann-Antenbrink, M. *et al.*, Enhancement of the efficiency of non-viral gene delivery by application of pulsed magnetic field. *Nucleic Acids Research*, 2006, **34**, e40.
- Galuppo, L. D., Kamau, S. W., Steitz, B., Hassa, P. O., Hilbe, M., Vaughan, L. *et al.*, Gene expression in synovial membrane cells after intraarticular delivery of plasmid-linked superparamagnetic iron oxide particles—a preliminary study in sheep. *Journal of Nanoscience and Nanotechnology*, 2006, **6**, 1–12.
- Rüfenacht, D., Doelker, E., Jordan, O., Chastellain, M., Petri-Fink, A. and Hofmann, H., Injectable superparamagnetic nanoparticles for treatment by hyperthermia and use for forming an hyperthermic implant, EP1883425, 2005.
- Juillerat F., Self-assembled nanostructures prepared by colloidal chemistry Thesis 3399, EPFL, 2005.
- Juillerat, F., Bowen, P. and Hofmann, H., Formation and drying of colloidal crystals using nanosized silica particles. *Langmuir*, 2006, **22**, 2249–2257.
- Brinker, J. and Scherer, G. W., *Sol–gel Science: The Physics and Chemistry of Sol–gel Processing*. Academic Press Inc., San Diego, 1990.
- Scherer, G. W., *Journal of Non-Crystalline Solids*, 1989, **109**, 171.
- Kukreja, N., Onuma, Y., Daemen, J. and Serruys, P. W., The future of drug-eluting stents. *Pharmacological Research*, 2008, **57**, 171–180.
- Braginsky, L., Shklover, V., Hofmann, H. and Bowen, P., High-temperature thermal conductivity of porous Al<sub>2</sub>O<sub>3</sub> nanostructures. *Physical Review B*, 2004, **70**, 134201.
- Braginsky, L., Lukzen, N., Shklover, V. and Hofmann, H., High temperature phonons thermal conductivity of nanostructures. *Physical Review B*, 2002, **66**, 134203.
- Belaroui, K., Rapillard, G., Bowen, P., Hofmann, H. and Shklover, V., Nanocrystalline coating by electrophoretic deposition (EPD). *Key Engineering Materials*, vol. 206–213. Trans Tech Publications, Uetikon-Zuerich, Switzerland, 2002, pp. 519–522.
- Bowen, P., Hofmann, H., Staiger, M., Steiger, R., Brugger, P.-A. and Peterzell, K., Colloidal processing of nanoceramic powders for porous ceramic film applications. *Key Engineering Materials*, vol. 206–213. Trans Tech Publications, Uetikon-Zuerich, Switzerland, 2002, pp. 1977–1980.
- Juillerat, F., Solak, H. H., Bowen, P. and Hofmann, H., Fabrication of large-area ordered arrays of nanoparticles on patterned substrates. *Nanotechnology*, 2005, **16**, 1311–1316.